Harmonic Iron Loss Analysis of Rotating Machines: Practical Macro Modeling for Stress and Hysteresis

Katumi Yamazaki
(Chiba Institute of Technology)

In this symposium, I present harmonic iron loss analysis of rotating machines that considers effects of multi-axial mechanical stress and hysteresis phenomenon by introducing practical macro modeling.

First, the effect of the multi-axial stress on the loss is investigated by material experiments. An approximated modeling, which requires only the measured loss with uniaxial stress, is also introduced. Fig. 1 shows the experimental system [1], in which arbitrary 2-axial stress can be imposed on the specimen of an electrical steel sheet by the actuators noted 1 and 2. The magnetic field is applied along the direction of the force produced by actuator 1. The specimen is an electrical steel sheet with 3% silicon.

The hysteresis loss and the eddy current loss including the excess loss are separated from the measured total core losses at 50 Hz and 200 Hz. Fig. 2 shows the results. It is revealed that both the eddy current and hysteresis losses are affected by multi-axial stress. These losses become maximum when the compressive (minus) σ_1 and tensile (plus) σ_2 are imposed.

This experiment cannot be always carried out for practical design procedure of rotating machines. Approximated modeling is strongly desired. To obtain the approximated multi-axial stress effects, the single axial equivalent stress σ_{eq} has been proposed.

Following expression was derived under the assumption that a same magneto-elastic energy leads to a same characteristics of the magnetic materials [2]:

$$\sigma_{eq} = \frac{3}{2}\vec{h}.\boldsymbol{s}.\vec{h} \qquad (1)$$

where $\vec{h}$ is the unit vector along the magnetic field direction, $\boldsymbol{s}$ is the deviatoric part of the stress tensor expressed by σ_1 and σ_2. It is assumed that the variation in core loss with single σ_{eq} along the magnetic field direction is identical to that with multi-axial σ_1 and σ_2. Therefore, the effect of the multi-axial stress can be estimated only by (1) and the experiment, in which a uniaxial stress is simply imposed along the flux direction.

Fig. 3 shows the calculated variation in the losses only from the measured loss $W(\sigma_1,0)$ by single axial σ_1 and the equivalent stresses. It is confirmed that the calculated result well express the measured eddy current and hysteresis losses in Fig. 2.

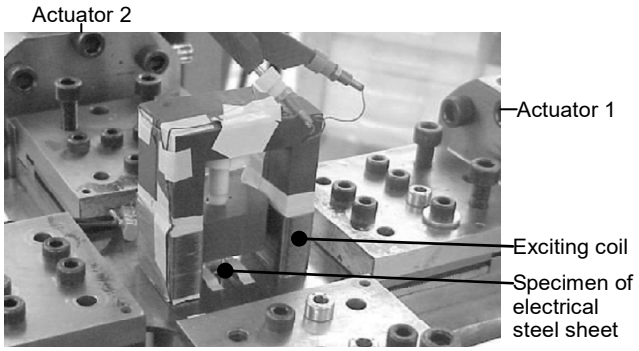

Fig. 1. Experimental system for effect of multi-axial stress[1].

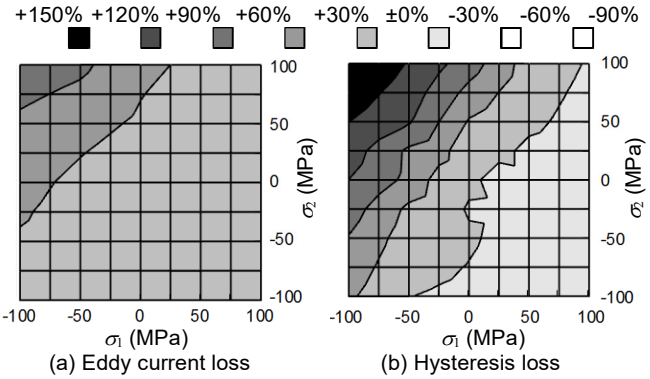

Fig. 2 . Measured variation in losses with multi-axial stress.

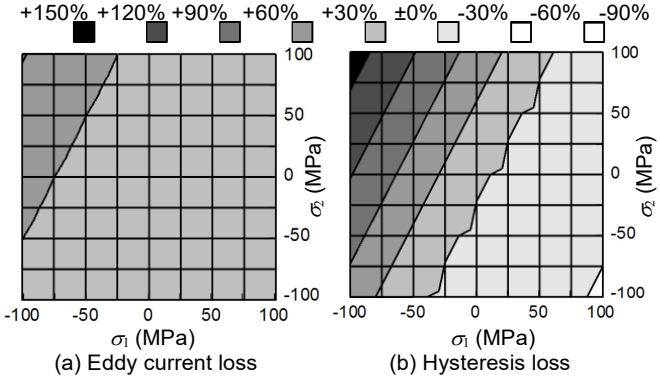

Fig. 3. Calculated losses by $W(\sigma_1,0)$ and σ_{eq} by (1)

Next, a practical hysteresis modeling including minor loops is proposed [3]. Fig. 4 shows the concept of this model. The minor loops are approximately determined form the several curves of major loops. Fig. 5 shows the experimental verification of this model by a single sheet test of an electrical steel sheet. The accuracy of the model is confirmed.

Finally, the proposed material modeling is applied to the loss calculation of a 100 kW class interior permanent magnet synchronous motor driven by a PWM inverter (5 kHz carrier). The 2D finite element analysis is carried out due to following equation.

$$\nabla \times \left(\frac{1}{\mu} \nabla \times \boldsymbol{A} \right) = \nabla \times \boldsymbol{H}_{eddy,ave} + \nabla \times \boldsymbol{H}_{hys,ave} \quad (2)$$

where μ is the permeability, $\boldsymbol{A}$ is the magnetic vector potential, $\boldsymbol{H}_{eddy,ave}$ and $\boldsymbol{H}_{hys,ave}$ are the reation field caused by the eddy currents and hysteresis phenomenon in the core, which are averaged along the thickness of electrical steel sheets. $\boldsymbol{H}_{eddy,ave}$ is determined by coupling 1D nonlinear time stepping analysis along the thickness of the electrical steel sheet in the core. $\boldsymbol{H}_{hys,ave}$ is determined by the presented hysteresis model by considering the effect of the stress due to (1).

Fig. 6 shows the calculated flux density waveform at the top of a stator tooth of the motor. The waveform includes high-frequency carrier harmonics. Fig. 7 shows the calculated hysteresis loops, which includes a considerable number of minor loops. It is observed that the differential permeability of the minor loops is considerably smaller than that of the B-H curve used in the conventional analysis. Fig. 8 shows the experimental and calculated iron losses. The accuracy is improved by the proposed method due to the correct estimation of skin effect.

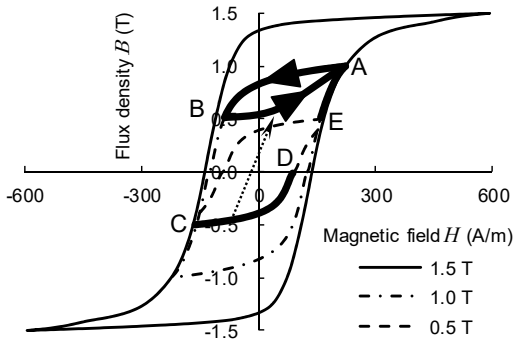

Fig. 4. Minor hysteresis loop modeling.

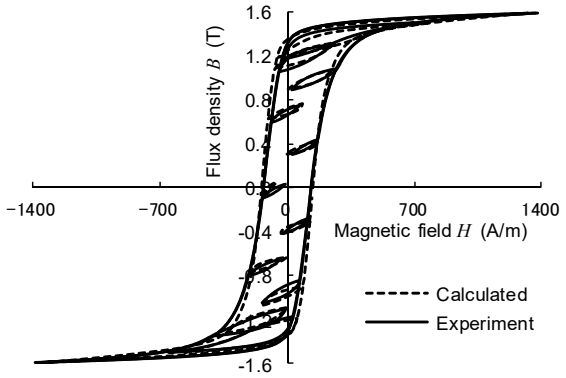

Fig. 5. Experimental verification of hysteresis modeling.

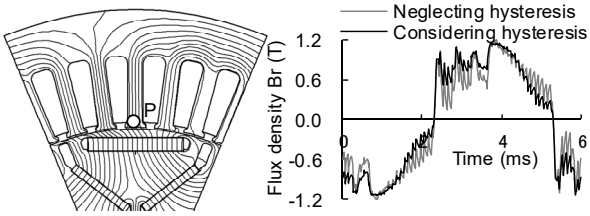

Fig. 6. Calculated flux density waveform (2500 r/min, 88A)

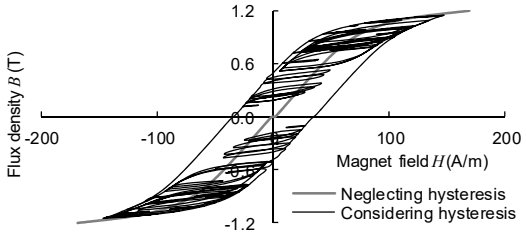

Fig. 7. Calculated hysteresis loop (2500 r/min, 88A).

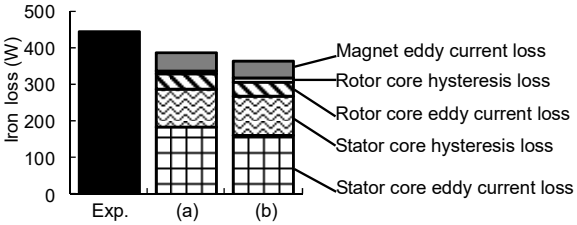

Fig. 8. Experimental and calculated iron losses (2500 r/min, 88A).
(a):Considering hysteresis, (b):Neglecting hysteresis

Reference

1) M. Rekik, O. Hubert, and L. Daniel, "Influence of a multiaxial stress on the reversible and irreversible magnetic behavior of a 3% Si-Fe alloy", *Int. J. Applied Electromagnetics and Mechanics*, vol. 44, no. 3, 4, pp. 301-315, 2014.

2) L. Daniel and O. Hubert, "An equivalent stress for the influence of multiaxial stress on the magnetic behavior," *J. Applied Physics*, vol. 105, 07A313, 2009.

3) K. Yamazaki and Y. Sakamoto, "Electromagnetic field analysis considering reaction field caused by eddy currents and hysteresis phenomenon in laminated cores," *IEEE Trans. Magn.*,vol.59, no. 3, 1300294, 2018.